DALTON

Thiophene-linked azacryptand sites for dicopper and disilver; thiophene sulfur as an inert spacer?*

Michael G. B. Drew,[a] Charles J. Harding,[b] Oliver W. Howarth,[d] Qin Lu,[c] Debbie J. Marrs,[b,c] Grace G. Morgan,[b,c] Vickie McKee[c] and Jane Nelson[b,c]

[a] *Chemistry Department, The University, Reading RG6 2AD, UK*
[b] *Chemistry Department, Open University, Milton Keynes MK7 6AA, UK*
[c] *School of Chemistry, Queens University, Belfast BT9 5AG, UK*
[d] *Chemistry Department, University of Warwick, Coventry CV4 7AL, UK*

Two disilver cryptates of the thiophene-spaced azacryptand hexa Schiff bases $N[(CH_2)_nN{=}CHRHC{=}N(CH_2)_n]_3N$ (n = 2 or 3, R = thiophene-2,5-diyl) and with the dicopper(I) cryptate where n = 2 have been structurally characterised. The dinuclear separation increases by 0.36 Å on going from the disilver complex of the n = 2 cryptand, to the n = 3 analogue, with that in the dicopper(I) cryptate intermediate, but little difference in cryptand conformation is observed in the three complexes. Proton NMR spectra show three-bond (H–C=N–Ag) coupling of each imino CH proton to ^{109,107}Ag, confirmed by an ^{109}Ag insensitive nuclei enhanced by polarisation transfer experiment. No copper(II) cryptates were obtained with the hexa(Schiff-base) cryptands. The analogous octaamino compounds generate dicopper(II) cryptates which accommodate bridging anions in cascade fashion, with a bridging disposition collinear, Cu–NNN–Cu, in the μ-azido-, but non-linear, Cu–O(H)–Cu, in the μ-hydroxo-cryptate. Both the hexa(Schiff-base) and octaamino cryptates are very similar to inert-spacer azacryptates and give no evidence for hemico-ordination of thiophene sulfur.

Sulfur donors are known to be good ligands for Group 11 cations, particularly in their low oxidation states. Azacryptands are also potentially valuable hosts for such cations, and where these contain S-donors in the linker units it is of interest to discover what effect any potential sulfur co-ordination or hemico-ordination may have. It is now generally recognised that sulfur ligation of copper plays an important role in metalloenzyme chemistry,[1] particularly in the control of redox potential. Long Cu–S (methionine) contacts in the range 2.7–3.2 Å, thought of as hemico-ordinate, are of particular current interest, as protein-engineering studies suggest that, notwithstanding an appreciable effect[2] on the redox and spectroscopic properties of the active site, in some such cases no co-ordination of S to Cu^{II} may be involved.[3] Thiophene sulfur is a good candidate for examining hemico-ordination as thiophene is not considered a strong donor ligand. In addition, the availability of four N-donors in addition to the thiophene S means that in thiophene-linked azacryptands any effect of hemico-ordinated or non-bonded but adjacent S atoms can be discerned by comparison with azacryptands which lack any potential donors in the spacer links.

The chemistry of copper encapsulated within the trigonal site defined by azacryptand ligands has been illustrated by studies[4–9] of dicopper cryptates of hexaimine macrobicycles which incorporate both innocent and potentially co-ordinating spacer units. In general, where donors, such as sp^3 N, N^- or O^- from the spacer groups are co-ordinated, there is enhanced thermodynamic stability of the +II state of copper, which may also be associated with distortion from trigonal geometry. In these sterically protected systems, however, the thermodynamically favoured aerobic oxidation may not be appreciable because of kinetic barriers to reaction,[10] which are general in the hexaimino cryptand hosts, unless deprotonation of potential donors in the linker group accompanies the oxidation. Within the more flexible octaamino hosts on the other hand interaction of dicopper(I) cryptates with dioxygen is generally observed.[5–7] This is normally rapid and the copper(I) cryptates may consequently be difficult to isolate and characterise.

Macrotricyclic ligands incorporating S-donors were studied as hosts for Group 11 cations over 20 years ago,[11] and although a number of macrocyclic thioether-[12] and thiophene[13]-based hosts for copper and silver have been examined since then, complexation studies of macrobicyclic hosts incorporating potential S-donors are rare.[14]

The furan-based cryptands L^3 and L^4 have proved useful hosts for copper and silver[6] cations, as well as for Group 2 cations and the $[Cu^{II}_2(OH)]^{3+}$ assembly. Replacement of the innocent 2,5-diimino furan linker by 2,5-diimino thiophene may be expected to have minimum effect on the chemistry of encapsulated copper cations unless the thiophene-S donor is engaged in co-ordination. In this paper we examine the capacity of the thiophene compound L^1 and its hydrogenated derivative L^2 ($=L^1$ + 12H) to accommodate copper and silver cations. In addition we have synthesised and characterised the disilver cryptate of L^5, analogous to L^1 except that the tetraaza caps are derived from tris-(3-aminopropyl)amine rather than tris-(2-aminoethyl)amine. The additional freedom in the larger cryptand L^5 might be expected to allow differentiation of contacts enforced by steric constraint from those consequent on electronic interactions.

Results and Discussion

Unlike the furan-based[15] cryptand L^3, L^1 is not readily made by direct condensation, but can be synthesised *via* the silver(I) template method[16] in near-quantitative yield as the disilver cryptate $[Ag_2L^1][O_3SCF_3]_2$ **1**. Compound L^5 is similarly made, generating $[Ag_2L^5][ClO_4]_2$ **2a**. Transmetallation of **1** with either Cu^I or Cu^{II} generates dicopper(I) salts $[Cu_2L^1][O_3SCF_3]_2$ **3** or $[Cu_2L^1][BF_4]_2$ **3a** in reasonable yield, but a more satisfactory product can be generated *via* direct template

* *Supplementary data available* (No. SUP 57144, 11 pp): magnetic susceptibilities. See Instructions for Authors, *J. Chem. Soc., Dalton Trans.*, 1996, Issue 1.

Non-SI units employed: G = 10^{-4} T, $\mu_B \approx 9.27 \times 10^{-24}$ J T^{-1}.

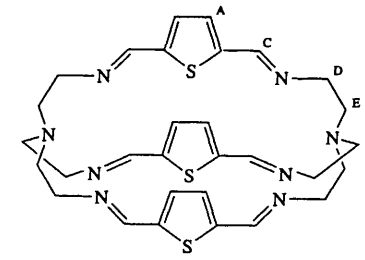

L^1

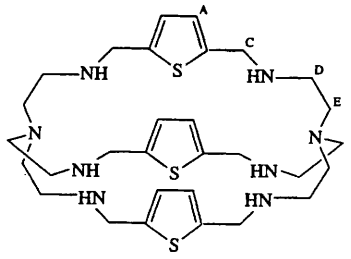

L^2

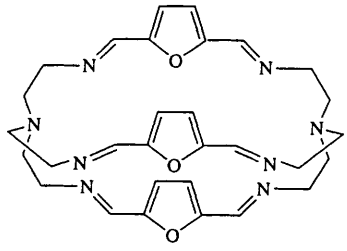

L^3

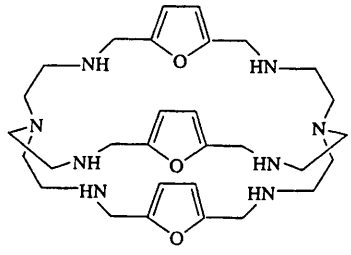

L^4

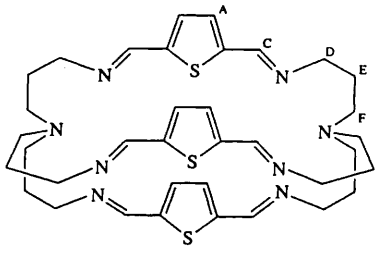

L^5

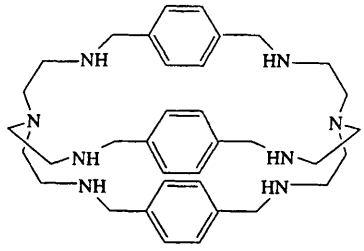

L^6

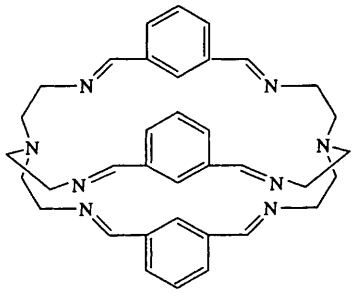

L^7

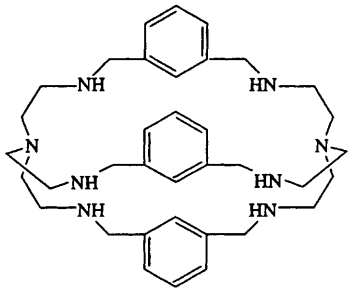

L^8

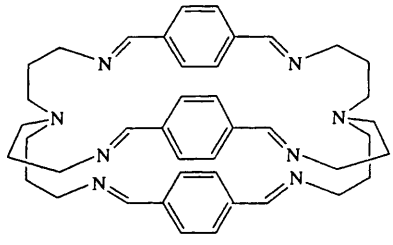

L^9

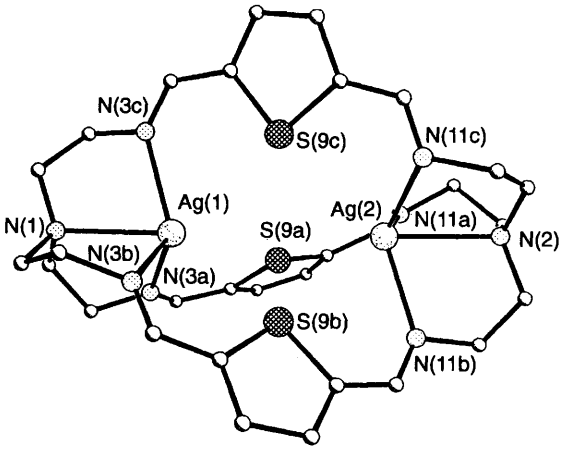

Fig. 1 Structure of the cation in complex **1**

reaction on Cu^I. Recrystallisation of **1**, **2a** or **3** yielded crystals (in the case of **2a** as the 1 : 1 ethanol solvate, hereafter referred to as **2**) suitable for X-ray crystallographic structure determination.

Crystal structure of disilver cryptates

Complex 1. The structure contains discrete cations and anions. In the $[Ag_2L^1]^{2+}$ cation the two silver atoms are encapsulated within the macrocycle at the two ends as shown in Fig. 1 which also illustrates the atomic numbering scheme. The Ag–N bridgehead nitrogen distances [2.51(2), 2.54(2) Å] are significantly longer than the Ag–N imine distances [2.29(2)–2.39(2) Å] (Table 1). The geometry around the metal atoms is unusual as all four nitrogen atoms are on one side of the metal. The N (bridgehead)–Ag–N (imine) angles are all between 73.3(6) and 75.6(6)°, while the (imine) N–Ag–N (imine) angles are between 110.0(7) and 116.3(6)°. In addition to these four bonds there are long contacts between the silver atoms and the thiophene sulfur atoms ranging from 3.20(1) to 3.30(1) Å. Were these contacts to be included, the metal co-ordination sphere would resemble a seven-co-ordinate capped octahedron with the bridgehead nitrogen in the capped position, the three imine nitrogen atoms in the capped face and the three sulfur atoms in

Table 1 Molecular dimensions (distances in Å, angles in °) in the metal co-ordination sphere for complex **1**

Ag(1)–N(1)	2.509(18)	Ag(2)–N(11c)	2.338(22)
Ag(1)–N(3a)	2.341(23)	Ag(1) · · · S(9a)	3.227(8)
Ag(1)–N(3b)	2.393(22)	Ag(1)–S(9b)	3.298(7)
Ag(1)–N(3c)	2.358(19)	Ag(1)–S(9c)	3.271(8)
Ag(2)–N(2)	2.537(20)	Ag(2)–S(9a)	3.268(7)
Ag(2)–N(11a)	2.288(20)	Ag(2)–S(9b)	3.197(8)
Ag(2)–N(11b)	2.313(18)	Ag(2)–S(9c)	3.245(7)
N(1)–Ag(1)–N(3a)	75.0(7)	N(2)–Ag(2)–N(11a)	73.3(6)
N(1)–Ag(1)–N(3b)	75.6(6)	N(2)–Ag(2)–N(11b)	75.0(6)
N(3a)–Ag(1)–N(3b)	110.5(7)	N(11a)–Ag(2)–N(11b)	110.0(7)
N(1)–Ag(1)–N(3c)	74.0(6)	N(2)–Ag(2)–N(11c)	75.2(7)
N(3a)–Ag(1)–N(3c)	114.9(6)	N(11a)–Ag(2)–N(11c)	113.1(7)
N(3b)–Ag(1)–N(3c)	114.8(7)	N(11b)–Ag(2)–N(11c)	116.3(6)

Table 2 Selected bond lengths (Å) and angles (°) for complex **2**

Ag(1)–N(2c)	2.280(4)	Ag(1)–N(2b)	2.304(4)
Ag(1)–N(2a)	2.334(4)	Ag(1)–N(200)	2.491(4)
Ag(1) · · · Ag(2)	5.0044(7)	Ag(2)–N(1a)	2.276(4)
Ag(2)–N(1c)	2.300(4)	Ag(2)–N(1b)	2.363(4)
Ag(2)–N(100)	2.484(4)		
N(2c)–Ag(1)–N(2b)	127.1(2	N(2c)–Ag(1)–N(2a)	123.99(14)
N(2b)–Ag(1)–N(2a)	108.74(14)	N(2c)–Ag(1)–N(200)	89.58(13)
N(2b)–Ag(1)–N(200)	91.35(13)	N(2a)–Ag(1)–N(200)	84.16(14)
N(1a)–Ag(2)–N(1c)	134.4(2)	N(1a)–Ag(2)–N(1b)	108.04(14)
N(1c)–Ag(2)–N(1b)	116.69(14)	N(1a)–Ag(2)–N(100)	91.23(13)
N(1c)–Ag(2)–N(100)	84.54(13)	N(1b)–Ag(2)–N(100)	84.98(13)

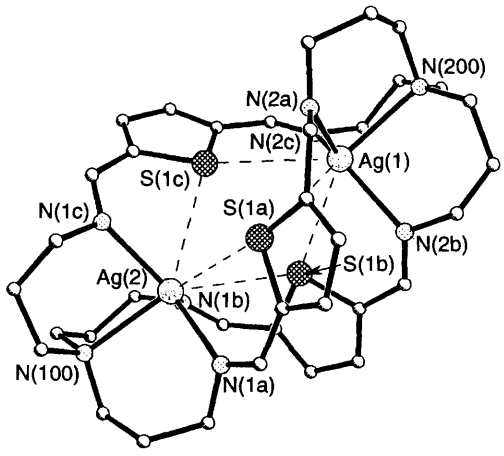

Fig. 2 Structure of the cation in complex **2**; dashed lines indicate the Ag · · · S distances of ≈3.22 Å

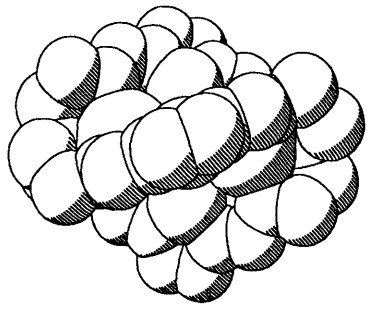

$[Ag_2L^1]^{2+}$

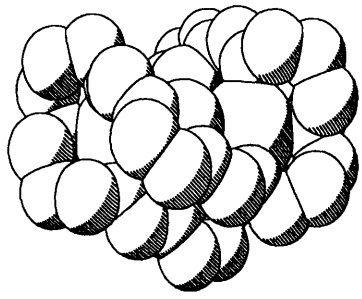

$[Ag_2L^5]^{2+}$

Fig. 3 Space-filling representation of the cations in complexes **1** and **2** showing helicity

the uncapped face. The Ag · · · Ag distance is 4.65 Å and the N · · · N bridgehead distance 9.69 Å.

Complex 2. This structure contains discrete $[Ag_2L^5]^{2+}$ cations, shown in Fig. 2, two ClO_4^- anions and a molecule of ethanol. As in **1** the silver atoms are ostensibly four-co-ordinate; each forms three bonds in the range 2.27–2.36 Å to the imine nitrogens with a longer contact to the bridgehead nitrogen at ≈2.49 Å (Table 2). The silver–imine distances are on average very similar to those in the smaller cryptate **1** whereas the silver–nitrogen-bridgehead distances are very slightly shorter. The positions of Ag(1) and Ag(2) relative to the imine plane are not identical: Ag(2) like the silver atoms in **1** sits inside the plane formed by the three imine nitrogens so that all four nitrogen donors are on one side of the metal cation; Ag(1) is not in the N_3 plane but slightly off it in the opposite direction so that it lies between the bridgehead atom and the three imino donors. Generally the silver atoms in **2** lie nearer the N_3 plane than in **1** and in consequence the N_{imine}–Ag–N_{imine} angles total almost 360° [N–Ag(1)–N 123.99(14), 127.1(2) and 108.74(14); N–Ag(2)–N 116.69(14), 134.4(2) and 108.04(14)°]. Distances from the imine plane in **2** are only 0.06 Å for Ag(1) and 0.12 Å for Ag(2) compared with 0.62 Å for both silver atoms in **1**.

The position of the silver atoms relative to the imine plane in complex **2** does not appear to affect the Ag–$S_{thiophene}$ distances which are comparable to those in **1** [average ≈3.21 for Ag(1) and ≈3.23 Å for Ag(2)]. These distances are on average (3.22 *vs.* 3.25 Å) slightly shorter than in the smaller cryptate **1**. Both the Ag · · · Ag 5.004(1) Å and N_{br} · · · N_{br} distance of ≈9.962 Å, however, are longer than in **1**; siting of Ag^+ closer to the N_3 plane contributes to an increased internuclear Ag · · · Ag distance, which is, however, less than expected because of the greater helicity (Fig. 3) of cryptand strands in **2**.

It is difficult to assess whether the Ag · · · S distances in complexes **1** and **2** represent genuine interactions, as the constraints of the ligand require the thiophene parts to be placed approximately in those positions, but it is striking that they are so similar in the different hosts. The increase in the Ag · · · Ag distance in **2** for example has not generated an increase in Ag · · · S distance. In other complexes where silver–thiophene co-ordinate bonds have been proposed, Ag–S distances of the order of 3.10 Å, *i.e.* >0.1 Å shorter than in these cryptates have been observed;[17] however it has to be remembered that the higher silver co-ordination numbers present in the cryptates would in any case be expected to generate longer Ag–S bonds.

In the structure[17] of a related disilver cryptate $[Ag_2L^3]^{2+}$ the silver ions were encapsulated in the macrobicycle at either end and each was bound to four nitrogen atoms. Compound L^3 is equivalent to L^1 except for the replacement of thiophene by furan; in $[Ag_2L^3]^{2+}$ the Ag · · · Ag distance is 3.145 Å and the Ag · · · O contact is ≈3.144 Å.

The conformation of the macrocycle L^1 in complex **1** is described by the torsion angles listed in Table 3(*b*). The three linkages between the two bridgehead atoms are similar. The conformations of free and co-ordinated L^3 are also illustrated by the torsion angles in Table 3. (Note that for free L^3 these are average values taken over the three linkages.) As can be seen the crucial change is that N(3)–C(4)–C(5)–S(9) is *cis* in $[AgL^1]^{2+}$ and $[AgL^3]^{2+}$ while the equivalent N–C–C–O torsion angle in $L^3 \cdot H_2O$ is *trans*. It seems likely that L^1 also has two different conformations, one in the free state with the imine nitrogens directed outwards and another when acting as host for metal cations. Further evidence for the generality of a 'divergent' conformation for free and 'convergent' conformation for co-ordinated azacryptands is provided by comparison of the crystal structure of $L^6 \cdot 6H_2O$ with that of its disilver cryptate.[16] It is interesting that a similar conformation to that found in L^6 is also found[15] in L^7 where the link is *m*-phenylene (torsion angles in Table 3). This strongly suggests that the metal-free conformation of L^1 would be the equivalent of that found for the crystal structures of the free cryptands L^3 and L^7.

Table 3 Torsion angles (°)

(*a*) Around the bridgehead nitrogens

	$[Ag_2L^1]^{2+}$	$[Ag_2L^3]^{2+}$
C(1b)–N(1)–C(1a)–C(2a)	−83.5	−86.8
C(1c)–N(1)–C(1a)–C(2a)	150.1	140.3
C(1c)–N(1)–C(1b)–C(2b)	−83.8	−82.0
C(1a)–N(1)–C(1b)–C(2b)	147.3	144.7
C(1a)–N(1)–C(1c)–C(2c)	−81.6	−83.2
C(1b)–N(1)–C(1c)–C(2c)	152.5	144.2
C(13c)–N(2)–C(13a)–C(12a)	−79.1	−82.2
C(13b)–N(2)–C(13a)–C(12a)	149.9	144.3
C(13a)–N(2)–C(13b)–C(12b)	−74.0	−86.1
C(13c)–N(2)–C(13b)–C(12b)	152.5	141.0
C(13b)–N(2)–C(13c)–C(12c)	−79.4	−88.4
C(13a)–N(2)–C(13c)–C(12c)	146.8	138.3

(*b*) Along each strand

	$[Ag_2L^1]^{2+}$			$[Ag_2L^3]^{2+}$				
	a	b	c	a	b	c	$L^3 \cdot H_2O$	L^7
N(1)–C(2)–C(3)–N(3)	−55.7	−61.0	−62.4	−60.4	−64.1	−64.8	73.4	75.5
C(2)–C(3)–N(3)–C(4)	−126.0	−115.7	−120.3	−99.2	−103.8	−109.1	−23.7	−122.7
C(3)–N(3)–C(4)–C(5)	−177.8	−174.0	−175.2	172.8	172.7	176.1	−178.6	−178.6
N(3)–C(4)–C(5)–X(9)	4.6	2.4	−7.4	8.6	7.4	2.5	175.8	173.3
X(9)–C(8)–C(10)–N(11)	8.8	12.4	3.8	6.6	2.9	3.0	−177.0	−173.8
C(8)–C(10)–N(11)–C(12)	−175.2	176.8	−175.8	172.7	174.2	174.5	177.0	−175.5
C(10)–N(11)–C(12)–C(13)	−109.7	−118.3	−111.8	−109.9	−95.7	−88.5	118.1	121.2
N(11)–C(12)–C(13)–N(2)	−62.6	−66.1	−57.3	−64.4	−59.5	−60.3	−72.9	−73.5

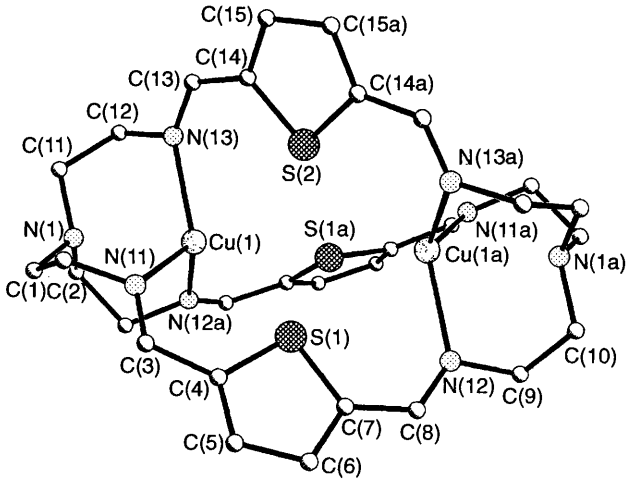

Fig. 4 Structure of the cation in complex **3**

Table 4 Selected bond lengths (Å) and angles (°) for complex **3**

Cu(1)–N(11)	2.180(11)	Cu(1)–N(12a^{I})	2.229(9)
Cu(1)–N(13)	2.232(10)	Cu(1)–N(1)	2.563(10)
Cu(2)–N(23^{II})	2.240(10)	Cu(2)–N(21^{II})	2.247(11)
Cu(2)–N(22)	2.270(10)	Cu(2)–N(2^{II})	2.514(11)
Cu(1) · · · Cu(1a^{I})	4.733(2)	Cu(2) · · · Cu(2a^{II})	4.826(2)
N(11)–Cu(1)–N(12a^{I})	113.9(3)	N(11)–Cu(1)–N(13)	113.8(3)
N(12a^{I})–Cu(1)–N(13)	112.4(3)	N(11)–Cu(1)–N(1)	74.4(3)
N(12a^{I})–Cu(1)–N(1)	74.9(3)	N(13)–Cu(1)–N(1)	75.1(3)
N(23^{II})–Cu(2)–N(21^{II})	116.3(4)	N(23^{II})–Cu(2)–N(22)	113.4(4)
N(21^{II})–Cu(2)–N(22)	111.7(4)	N(23^{II})–Cu(2)–N(2^{II})	75.1(4)
N(21^{II})–Cu(2)–N(2^{II})	76.1(4)	N(22)–Cu(2)–N(2^{II})	74.8(3)

Symmetry transformations used to generate equivalent atoms: I $-x + \frac{3}{2}, -y + 1, z$; II $-x + \frac{3}{2}, -y, z$.

Structure of $[Cu_2L^1][O_3SCF_3]_2$ 3

The asymmetric unit contains half of each of two independent $[Cu_2L^1]^{2+}$ cations, along with two triflate anions (Table 4). Each cation sits on a two-fold rotation axis which passes through the sulfur atom in one of the thiophene rings [S(2) or S(4)] and bisects the Cu–Cu vector. There is an approximate, non-crystallographic three-fold axis passing through the copper and bridgehead nitrogen atoms of each cation. Although the cations are very similar, there are some subtle differences which can probably be ascribed to packing effects, the most noticeable of which is the Cu · · · Cu distance [Cu(1) · · · Cu(1a) 4.733(2) and Cu(2) · · · Cu(2a) 4.826(2) Å]. In each case (Fig. 4) the copper ion is co-ordinated to the three imine nitrogen atoms and is displaced by *ca.* 0.5 Å from the plane of the three donors towards the centre of the cavity. The copper and bridgehead nitrogen atoms interact weakly [2.56(1) and 2.51(1) Å for Cu(1)–N(1) and Cu(2)–N(2), respectively] and the copper–thiophene sulfur distances are in the range 3.17–3.31 Å.

There are no significant cation–cation interactions and the triflate anions do not interact with the cation, however there is a relatively short contact between one fluorine atom and its symmetry equivalent (2.84 Å).

Although complexes **1** and **3** are not isostructural, no major differences of co-ordination site geometry or cryptand conformation with each other or with **2** are evident. In **3** the M–N (imino) distances are >0.1 Å less than in the silver structures **1** and **2**, as befits the smaller cationic radius of Cu^{I}. However the M–N_{br} distances are almost identical to those in **1** and **2** suggesting that this contact is a matter of steric necessity. The M · · · S (thiophene) contacts are virtually identical (average 3.24 *vs.* 3.25 Å) to those made by Ag to sulfur in **1**, and although just less than van der Waals contact distance are 0.2–0.3 Å longer than in an analogous dicopper(I) thiophene-based macrocyclic complex.[13] This suggests that if any Cu · · · S interaction is to be proposed it must be very weak. The Cu · · · Cu distance in **3**, at 4.73–4.83 Å, is somewhat longer (by 0.1–0.2 Å) than the corresponding Ag · · · Ag distance in **1**. The N_{br} · · · N_{br} is also (at 9.859, 9.855 Å) somewhat longer than in **1**; it compares with 9.69, 8.53 and 9.96 Å for Ag_2L^1, Ag_2L^3 and Ag_2L^5 cryptates and a distance of more than 10 Å for the analogous metal-free cryptands.

In conclusion, both L^1 cryptates have metal ions sited outside the N_3 plane, displaced toward the centre of the cavity, while in the L^5 cryptate the cations have relaxed back into the N_3 plane with consequent increase of the Ag · · · Ag internuclear

distance. In the other disilver cryptates we have studied the distance of Ag^+ from the N_3 imine plane varies from 0.72 Å (away from the cap) for $[Ag_2L^3]^{2+}$ to −0.19 Å (toward the cap) in $[Ag_2L^9]^{2+}$. The difference in position of the metal cation in **1** as against **2** has no effect on $M\cdots N_{br}$ or $M\cdots S_{thiophene}$ distances.

NMR spectra of the Ag_2 and Cu^I_2 cryptates

Proton NMR spectra of the L^1 cryptates (Table 5) prove sensitive to small changes in ligand geometry. The disilver complex **1** has a simple room-temperature ^1H NMR spectrum. The highest δ resonance, H_C, takes the form of a closely spaced doublet corresponding to the imino protons, while the thiophene protons, H_A, generate just one signal. The methylene signals are broadened and fluxional; H_D, just below coalescence at ambient temperatures, gives a pair of broad peaks (with coupling washed out) corresponding to axial and equatorial resonance, while for H_E the axial/equatorial components are not resolved and this proton still generates a reasonably sharp unsplit singlet, of intensity = 4 H per proton strand. As the temperature is reduced the methylene coupling pattern becomes discernible and by 233 K the H_D protons are seen as well separated axial triplet and equatorial doublets while the H_E axial and equatorial resonances overlap, generating a multiplet.

The spectrum of complex **2a** at low temperature is more complex than that of **1**, with two separate imino CH and two separate (and mutually coupled) thiophene CH resonances in 1:1 ratio indicating an unsymmetric disilver cryptate with two different silver sites (Table 5). [There is also evidence for a symmetric disilver cryptate as a minor (≈10%) conformer.] The observation of coupling (≈3 Hz) between thiophene protons in the major conformer confirms inequivalence of these protons which is only possible in an unsymmetric conformation. Each of the imino resonances is split into a doublet with different (6–9 Hz) separation. Partial analysis of the methylene resonances confirms the existence of two inequivalent halves of the molecule, which generates a separate resonance for each of the twelve methylene protons in the strand. However, although high δ signals can be attributed to methylene protons α to the imine nitrogen, there is too much overlapping to allow full assignment of the other methylene resonances.

In the ^1H NMR spectrum (Table 5) of the dicopper(I) cryptate **3a** no splitting of the imino signal is evident, showing that the conformation in this case is symmetric and the imino proton uncoupled. The methylene region is well resolved and shows no signs of fluxionality; both major (axial/axial) and minor (axial/equatorial, *etc.*) vicinal couplings can be discerned at ambient temperatures. Also, no overlap of axial and equatorial resonances exists to complicate the H_E coupling pattern. Differences in the chemical shift of analogous resonances in the ^1H NMR spectra of **1** and **3a** confirm that the lack of isomorphism of these complexes in the solid state extends to their solution conformations. Another inference from the highly resolved spectrum of **3a** is that exchange of copper(I) cations between solvated and cryptated states is slow on the NMR time-scale.

Despite the minor conformational differences the co-ordination sites for the cations in **1**, **2a** and **3a** are very similar, which suggests that the splitting of the imino resonance in **1** does not originate in any asymmetry of the cryptand host, which would generate inequivalent imino and thiophene protons. Instead we look for an explanation in a coupling process, the more so because the splittings observed are independent of spectrometer frequency. The most likely is three-bond coupling of the imino proton to the $S = \frac{1}{2}$ isotopes $^{109,107}Ag$. Similar couplings have been observed[6,7] for other disilver cryptates of the series, as well as some acyclic silver imine complexes[18] We therefore sought confirmation of the presence of ^{109}Ag coupling for this and other disilver cryptates *via* a $\{^1H-^{109}Ag\}$ INEPT (insensitive nuclei enhanced by polarisation transfer) experiment, the results of which are illustrated in Fig 5.

Direct observation of insensitive nuclei such as ^{109}Ag becomes possible *via* the INEPT sequence whenever the nucleus shows a resolved ^1H scalar coupling[18] [for these cryptates the $^3J(^{109}Ag-^1H)$ coupling is around 8 Hz]. The INEPT experiment allows evaluation both of the chemical shift of ^{109}Ag and of the three-bond coupling constant, although in these systems the breadth of the ^{109}Ag resonance makes it preferable to use the ^1H coupling for evaluation of $^3J(^{109,107}Ag-^1H)$ (Table 5). For comparison with $[Ag_2L^1]^{2+}$, we also examined the INEPT spectrum of $[Ag_2L^3]^{2+}$, which displayed similar shift and coupling of the imino CH resonance.[6] Owing to low solubility, we were unable to obtain an INEPT spectrum for **2**, but the imine splitting in this case may be assigned to $^3J(^{109,107}Ag-^1H)$ by extrapolation from Ag_2L^1 and Ag_2L^3. Few other ^{109}Ag spectra are available for comparison; an acyclic system with similar ligation[18] shows chemical shifts somewhat shielded (at δ ≈ 580 from 2 mol dm^{-3} $AgNO_3$) *vs.* those (δ 610.0 for **1** and 609.7 for $[Ag_2L^3]^{2+}$) seen for the cryptates.

Observation of three-bond coupling to silver confirms the absence of any dynamic process involving Ag^+ and emphasises the kinetic inertness toward decomplexation of these cryptates. This is especially noticeable within the thiophene-linked cryptands where ^{109}Ag coupling is observed throughout the fluid range of the deuterioacetonitrile solvent. Kinetic barriers to decomplexation are rarely high in silver complexes, so this observation is of potential significance, for example, in connection with silver radionuclide transport.

Although such direct confirmation is not available for complex **3a** because of the quadrupolar nature of the $^{63,65}Cu$ nuclei, the kinetic barrier to decomplexation appears greater than in **1**, to judge by the sharply resolved 'frozen-out' nature of the methylene spectrum throughout the fluid range of the acetonitrile solvent. So L^1 is a good host for Cu^I. It, however, shows no tendency to accommodate Cu^{II}, even as the μ-hydroxo-dicopper assembly found in other iminocryptands.[6,7] Cyclic voltammetry of **3a** shows an irreversible two-electron oxidation wave[10] at relatively positive potential (+480 V *vs.* ferrocene–ferrocenium) exceeded in the iminocryptand series only by the second (Cu_2L^{3+}–Cu_2L^{4+}) oxidation potential of L^7. A geometry unfavourable to the $[Cu_2(OH)]^{3+}$ assembly may play a part in the failure of L^1 and L^5 to generate dicopper(II) cryptates.

Dicopper complexes of L^2

In order to achieve the dicopper(II) state we reduced the hexaimino ligand L^1 to the octaamino form L^2, anticipating that the harder sp^3-N donors would stabilise the higher oxidation state, while the greater flexibility of L^2 would simultaneously ensure less restrictive co-ordination site geometry. On treating L^2 with copper(I) salt an air-sensitive cream solid $[Cu_2L^2][ClO_4]_2$ **4** was isolated which acquired a greenish colour on standing in air over a period of weeks, but within minutes in solution. Cyclic voltammetry of **4** is, like that of **3a**,[10] irreversible, but the ≈0.5 V more negative (at E_c = 0.03 V *vs.* ferrocene–ferrocenium) potential indicates the expected enhanced stability of the +II state. When L^2 is treated with Cu^{II} under basic conditions a green microcrystalline product $[Cu_2L^2(OH)][ClO_4]_3\cdot H_2O$ **5** is obtained. The dimethylformamide (dmf) glass ESR spectrum of **5** gives no indication of large zero-field splitting effects, consisting only of a single g = 2.1 signal with poorly resolved (≈80 G) hyperfine structure and a weak (10^{-2}–10^{-3} times intensity of $g \approx 2$ signal) half-field signal which lacks hyperfine structure. The temperature dependence of the magnetic susceptibility accords

Table 5 Proton NMR spectral data for hexaimino cryptates[a]

Complex	Solvent	T/K	Imino CH (H_C)	$^3J(^{109}Ag–^1H)$/Hz	Thiophene CH (H_A)	Methylene (H_D, H_E, H_F)
1 $[Ag_2L^1][O_3SCF_3]_2$	CD_3CN	294	8.68 (d)	8.41	7.64 (s)	3.80 (br s),[b] 3.45 (br s),[b] 2.91 (br s),[c] 2.89 (br s)[c]
	CD_3CN	233	8.65 (d)	8.65	7.63 (s)	3.76 (t),[b,d] 3.38 (d),[b,d] 2.86 (m)[b,e]
3a $[Cu_2L^1][BF_4]_2$	CD_3CN	294	8.61 (s)	—	7.58 (s)	3.66 (t),[b,f] 3.48 (d),[b,f] 3.07 (d),[c,f] 2.83 (t)[c,f]
2a $[Ag_2L^5][ClO_4]_2$	$CDCl_3$	295	8.59 (d)	7.83	7.57 (s)	3.64 (br t), 3.46 (br t), 2.77 (vbr s), 2.35–1.92 (m)
	CD_2Cl_2	193	8.55 (d)	6.45	7.52,[g] 7.48[g]	3.72 (br d), 3.58 (br t), 3.39 (br d), 3.17 (br m), 2.35 (m)
			8.48 (d)	8.86		
	$(CD_3)_2CO$	193	8.85 (d)	4.52	7.81 (d),[g] 7.73 (d)[g]	*h*
			8.78 (d)[i]	8.92		
			8.73 (d)[j]	8.77[j]	7.69 (s)[j]	

[a] 400 MHz spectrum, shifts in ppm from $SiMe_4$; s = singlet, d = doublet, t = triplet, m = multiplet, br = broad. [b] H_D. [c] H_E. [d] $J(H_{ax}H_{ax}) \approx 12$ Hz. [e] H_{ax},H_{eq} overlapped. [f] $J(H_{ax}H_{ax}) \approx J(H_{ax}H_{eq}) \approx 12$ Hz. [g] $^3J(H_AH_{A'}) \approx 3.8$ Hz. [h] Complex unassignable pattern. [i] Shows small ^4J to $H_{D(eq)}$. [j] Minor symmetric conformer.

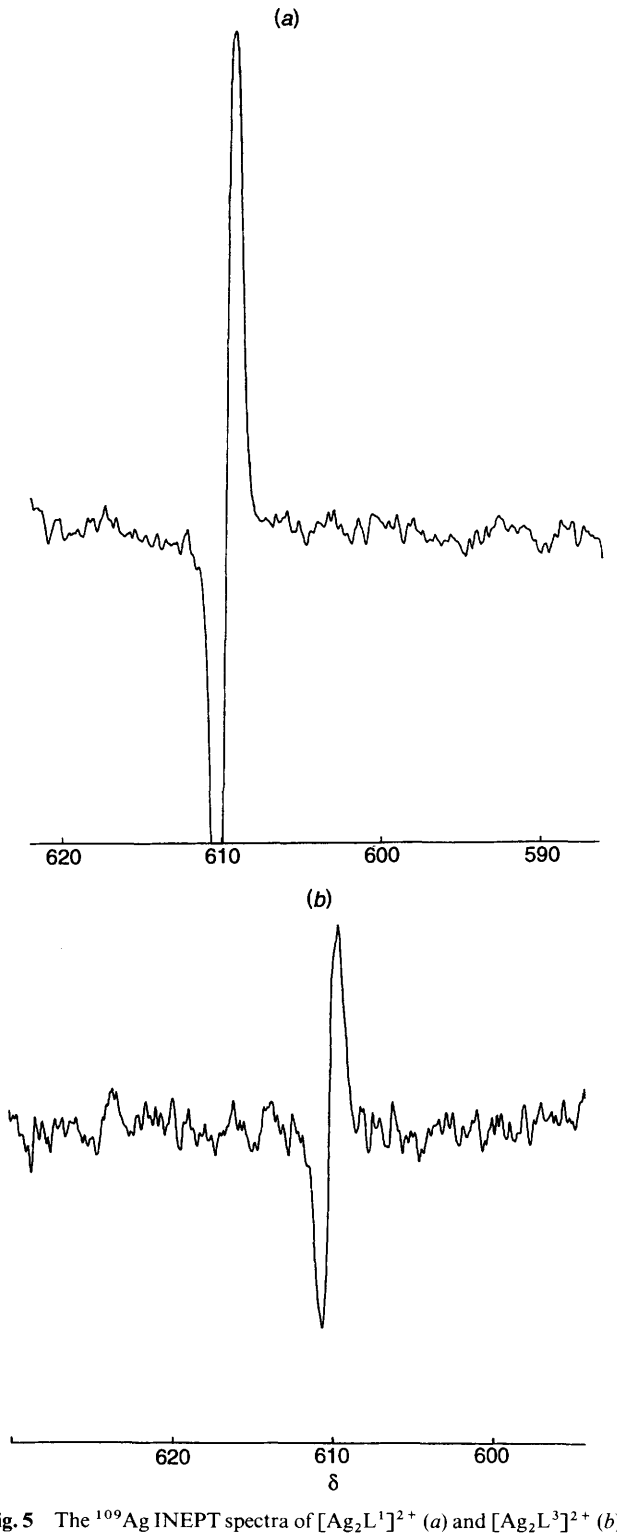

Fig. 5 The ^{109}Ag INEPT spectra of $[Ag_2L^1]^{2+}$ (*a*) and $[Ag_2L^3]^{2+}$ (*b*)

with this finding, revealing a magnetic exchange parameter (see Experimental section) of $2J = -72$ cm^{-1}. This is less than one tenth that found where the copper(II) paramagnets are linearly disposed, but similar to that found in $[Cu_2L^8(OH)]^{3+}$ where steric consequences are expected to derive from the projection of the α-aromatic CH into the cryptand cavity. In the case of **5** the reason for apparent non-linearity of the singly bridged $[Cu_2(OH)]^{3+}$ assembly could be a similar steric hindrance.

As with the other aminocryptands, L^4 and L^8, a single triatomic imidazolate or azido bridge is readily accommodated between the copper(II) ions. Moderate antiferromagnetic interaction ($-2J = 112$ cm^{-1}) is exhibited in the μ-imidazolate dimer $[Cu_2L^2(im)][O_3SCF_3]_3$ **6**, and there is ESR spectral evidence (Fig. 6) of thermal accessibility of the excited triplet state. A monoazido-bridged complex $[Cu_2L^2(N_3)][ClO_4]_3$ **7** having spectroscopic properties characteristic of a collinear M–NNN–M assembly[4,6,7] was obtained on treatment of $[Cu_2L_2(OH)]^{3+}$ with 1 equivalent of NaN_3. This complex shows an unusually high infrared $\nu_{asym}(N_3^-)$ absorption at 2211 cm^{-1}, an unusually low ligand-to-metal charge-transfer absorption (a broad strong band, appearing only in the Nujol mull spectrum, which suggests some decomposition in solution) centred around 465 nm and an X-band ESR spectrum (Fig. 7) extending over 5–6 kG with the most intense feature close to $g = 8$, too high a value to be attributed to a half-band signal, and thus tentatively assigned as the low-field D_z component. The intensification of the low-field component of D_z may be an artefact of the large axial zero field, which is of the same order as the microwave quantum. The Q-band spectrum.[19] currently under investigation, does not show any relative intensification of the low-field D_z component.

As described above, the behaviour of L^2 as host for dicopper(II) is very similar to the other aminocryptands L^4 and L^8; the only host-related difference is the tendency of $[Cu_2L^2(OH)]^{3+}$ to turn brown over time. Magnetic susceptibility measurements on an aged brown product do not indicate the presence of a significant diamagnetic component, so despite an accessible redox potential the change cannot be a simple autoreduction. The FAB mass spectra suggests that the brown product contains additional mass corresponding to OH^- or water, but we are at present unable to identify the site of attachment.

The conclusion from the similar behaviour of dicopper(II) cryptates of L^2, L^4 and L^8 is that the N_4 site controls the co-ordination behaviour and that the proximity of thiophene sulfur to the guest cations in these azacryptand hosts is not responsible for any significant changes in properties which could be associated with its co-ordination or hemico-ordination. The thiophene link is thus best considered as an inert spacer in these cryptates.

Experimental

Template synthesis

$[Ag_2L]X_2$ 1 (L = L^1, X = CF_3SO_3) and 2, 2a (L = L^5, X = ClO_4). 2,5-Diformylthiophene[21] and tris(3-aminopropyl)amine[22,23] were prepared by literature methods; tris(2-aminoethyl)amine (tren) was from Janssen and used without further purification.

2,5-Diformylthiophene (0.42 g, 0.003 mol) was dissolved in methanol (100 cm^3) and filtered into a solution of silver nitrate (0.376 g, 0.003 mol) in methanol (100 cm^3). A solution of the appropriate amine (0.003 mol) in methanol was added dropwise over 1 h to the stirred yellow solution at 50 °C. The solution was stirred at 50 °C for 1 h before black silver powder was filtered off to leave a clear yellow solution. The counter ion X was supplied as its sodium or lithium salt (0.006 mol) in methanol (75 cm^3). A microcrystalline product was filtered off in 70–90% yield, and recrystallised from MeCN–EtOH to generate X-ray diffraction-quality crystals, in the case of **2** as the 1:1 EtOH solvate. FAB mass spectrum: **1**, *m*/*z* 969 [$Ag_2L(CF_3SO_3)$, 67] and 711 (AgL 100); **2**, 1004 [$Ag_2L(ClO_4)$, 15], 904 (Ag_2L, 14) and 796 (AgL, 33%). Electrospray mass spectrum for **2**: *m*/*z* 1003 [$Ag_2L(ClO_4)$, 40], 907 (Ag_2L, 8), 896 [$AgL(ClO_4)$, 32] and 796 (AgL, 32%). Microanalytical data for these and other complexes are given in Table 6.

$[Cu_2L^1][BF_4]_2$ 3a. 2,5-Diformylthiophene (0.42 g, 0.003 mol) was dissolved in EtOH (50 cm^3) at room temperature then tren (0.3 cm^3, 0.002 mol) in EtOH (10 cm^3) was added dropwise. After bubbling N_2 for 10 min $[Cu(MeCN)_4]BF_4$ (0.63 g, 0.002

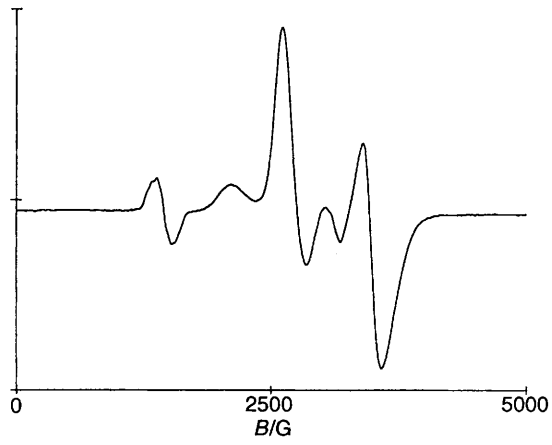

Fig. 6 X-Band ESR spectrum of complex **6**; dmf glass, 160 K

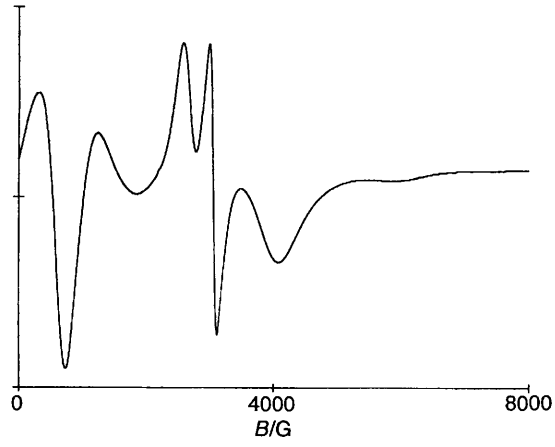

Fig. 7 X-Band ESR spectrum of complex **7**; polycrystalline, 160 K

mol) in deoxygenated MeCN (30 cm^3) was added. The volume was reduced under N_2 until an orange solid precipitated in 59% yield. FAB mass spectrum: *m/z* 819 [$Cu_2L(BF_4)$, 32], 732 (Cu_2L, 70) and 667 (CuL, 20%).

The triflate salt **3** used for X-ray crystallography was obtained by transmetallation of **1** with $Cu(O_3SCF_3)_2$ followed by recrystallisation from MeCN–EtOH.

L^2. The salt $[Ag_2L^1][O_3SCF_3]_2$ (4 g, 3.6 mmol) was brought to reflux in MeOH (300 cm^3). A large excess of solid $NaBH_4$ (10 g) was added in small portions. The resulting suspension was refluxed for 4 h. On cooling precipitated silver was filtered off and the solution reduced to dryness on a rotary evaporator. The residue was taken up in strong NaOH solution, extracted by chloroform, washed and dried. On pumping to remove last traces of solvent a waxy yellow solid was obtained in 60% yield. Mass spectrum: *m/z* = 616 (parent ion) (25% base peak at *m/z* = 110).

$[Cu_2L^2][ClO_4]_2$ 4. Compound L^2 (0.3 g, 0.0005 mol) was dissolved in deoxygenated EtOH (30 cm^3) and $[Cu(MeCN)_4]$-ClO_4 (0.32 g, 0.001 mol) in deoxygenated MeCN (30 cm^3) added. The mixture was heated at 40 °C under argon. On reducing the volume by bubbling Ar, $[Cu_2L^2][ClO_4]_2$ was obtained as a very pale green solid in 47% yield. It is reasonably stable in air over a period of months, but goes green in solution within minutes unless an inert atmosphere is provided.

$[Cu_2L^2(OH)][ClO_4]_3 \cdot H_2O$ 5. Compound L^2 (0.3 g, 0.0005 mol) was dissolved in EtOH (30 cm^3) at 50 °C and $Cu(ClO_4)_2 \cdot 6H_2O$ (0.37 g, 0.001 mol) in MeCN (20 cm^3) was added and the mixture stirred for 30 min at 50 °C, in the presence of pyrazole (0.0005 mol) as base. On reducing the volume, bright green microcrystals of product with ν_{OH} at 3571 cm^{-1} were obtained in 55% yield. On storage over a period of months these slowly turned brown. FAB mass spectrum: *m/z* 679 (CuL, 100), 741 (Cu_2L, 35), 779 [$CuL(ClO_4)$, 32] and 843 [$Cu_2L(ClO_4)$, 70%].

$[Cu_2L^2(im)][O_3SCF_3]_3$ 6. This complex was obtained analogously except that imidazole (0.0005 mol) was substituted for pyrazole; greeny blue needles of a product which lacked any ν_{OH} infrared absorption were obtained in 53% yield. FAB mass spectrum: *m/z* 891 [$Cu_2L(O_3SCF_3)$, 100], 960 [$Cu_2L(im)$-(O_3SCF_3), 70] and 1100 [$Cu_2L(im)(O_3SCF_3)_2$, 60%].

$[Cu_2L^2(N_3)][ClO_4]_3$ 7. Compound L^2 (0.3 g, 0.0005 mol) dissolved in MeOH (30 cm^3) was treated with $Cu(ClO_4)_2 \cdot 6H_2O$ (0.37 g, 0.0001 mol) in MeCN (20 cm^3) and NaN_3 (35 mg, 0.0005 mol) dissolved in the minimum (*ca.* 0.1 cm^3) of water was added. The green solution changed to brown from which gold-brown microcrystals of product were obtained in 57% yield. FAB mass spectrum: *m/z* 679 (CuL, 100), 741 (Cu_2L, 47) and 843 [$Cu_2L(ClO_4)$, 30%].

Crystallography

$[Ag_2L^1][O_3SCF_3]_2$ 1. *Crystal data.* $C_{32}H_{36}Ag_2F_6N_8O_6S_5$, M = 1118.73, monoclinic, space group $P2_1/c$, a = 14.340(8), b = 20.723(17), c = 15.213(14) Å, β = 110.4(1)°, U = 4237 $Å^3$, D_c = 1.75 g cm^{-3}, Z = 4, λ = 0.7107 Å, μ = 12.5 cm^{-1}, $F(000)$ = 2240.

A crystal of approximate size 0.30 × 0.30 × 0.30 mm was set up to rotate about the a axis on a Stoe Stadi2 diffractometer and data were collected at room temperature using Mo-Kα radiation *via* variable-width ω scan. Background counts were for 20 s and a scan rate of 0.03330 s^{-1} was applied to a width of [1.5 + (sin μ/tan θ)]. 4268 Independent reflections were measured of which 2396 with $I > 3\sigma(I)$ were used in subsequent refinement. No deterioration in the crystal was observed during the data collection. The structure was determined by the heavy-atom method. Non-hydrogen atoms in the cation were refined anisotropically. Hydrogen atoms were included in calculated positions and refined isotropically. Both triflate anions were disordered in a similar fashion in that the two orientations were located for the three fluorine atoms. These were refined on F with dimensional constraints and the two sets of fluorine atoms were given occupancies of x and $1 - x$ respectively. The two x values in the two triflates refined to 0.68 and 0.71 respectively. The sulfur and oxygen atoms were refined anisotropically but the carbon and fluorine atoms isotropically. No absorption correction was applied. Data were weighted $w = 1/[\sigma^2(F) + 0.003F^2]$. The final R value was 0.084 (R' = 0.095). Calculations were carried out using SHELX 76[20] together with some of our own programs on an Amdahl 5780 computer at the University of Reading. In the final cycles of refinement no shift/error ratio was greater than 0.3σ. In the final Fourier-difference maps the maximum and minimum peaks were 1.02 (located close to the metal atom) and −0.97 e $Å^{-3}$.

$[Ag_2L^5][ClO_4]_2 \cdot EtOH$ 2. *Crystal data.* Pale yellow needles, obtained by slow recrystallisation of complex **2a** from MeCN–EtOH. $C_{38}H_{54}Ag_2Cl_2N_8O_9S_3$, M = 1149.71, monoclinic, space group $P2_1/c$, a = 9.238(2), b = 22.388(3), c = 21.954(3) Å, β = 94.43(5)°, U = 4527.0(13) $Å^3$, Z = 4, μ(Mo-Kα) = 1.18 mm^{-1}, D_c = 1.687 Mg cm^{-3}, $F(000)$ = 2344, crystal dimensions 0.58 × 0.20 × 0.20 mm.

Data were collected at 123(2) K on a Siemens P4 four-circle diffractometer using graphite-monochromated Mo-Kα radiation (λ = 0.710 73 Å). Unit cell parameters were determined by non-linear least-squares refinements of 39 accurately centred reflections (10 < 2θ < 25°). 8489 Reflections were collected with 4 < 2θ < 50° using a scan width of 1.4° at 6° min^{-1} and equivalent reflections were merged to give 7958 (R_{int} = 0.0249)

Table 6 Analytical, spectral and magnetic data for disilver and dicopper cryptates

Cryptate	Analysis (%)			Selected IR data (cm^{-1})		Electronic spectra[a] (ct or d–d bands)
	C	H	N	ν(C=N)/ν(NH)	ν(X)[b]	
1 $[Ag_2L^1][O_3SCF_3]_2$	34.35 (34.2)	3.25 (3.20)	10.1 (10.4)	1631	1262, 1153, 1028	—
3a $[Cu_2L^1][BF_4]_2$	39.5 (39.8)	3.95 (4.00)	12.4 (12.4)	1610	1032	385 (4600)
2a $[Ag_2L^5][ClO_4]_2$	39.25 (39.2)	4.50 (4.85)	9.95 (10.15)	1620	1137, 1088, 1037	—
4 $[Cu_2L^2][ClO_4]_2$	38.0 (38.2)	5.15 (5.10)	11.45 (11.9)	3279	1091, 623	—
5 $[Cu_2L^2(OH)][ClO_4]_3 \cdot H_2O$	33.45 (33.45)	4.50 (4.75)	10.5 (10.4)	3523	1091, 623	380 (sh), 853 (250), 680 (230)
6 $[Cu_2L^2(im)][O_3SCF_3]_3$	34.3 (34.5)	4.00 (3.90)	11.2 (11.2)	3253	1255, 1165, 1030	360 (sh) (1900), 760 (490), 685 (430)
7 $[Cu_2L^2(N_3)][ClO_4]_3$	33.25 (33.2)	4.35 (4.45)	14.15 (14.2)	3261	2211,[c] 1100, 624	393 (3300), 853 (250), 680 (230) [d]465, 740, 900

[a] 10^{-3} mol dm^{-3} in MeCN; λ/nm (ε/dm^3 mol^{-1} cm^{-1}). [b] X = ClO_4, BF_4 or CF_3SO_3. [c] $\nu_{asym}(N_3^-)$. [d] Nujol mull; MeCN solution shows decomposition.

unique data which were used in the refinement. Crystal stability was monitored by recording three check reflections every 97 and a 3% decrease was observed. Solving by direct methods located both silver ions and 51 of the other 60 non-hydrogen atom positions. The remaining non-hydrogen atoms were found after isotropic full-matrix least-squares refinement on F^2 to give $R = 0.1787$. The two silver, three sulfur and all atoms in both ClO_4^- counter ions were then assigned anisotropic thermal parameters in a second least-squares refinement which reduced R to 0.0840. An empirical absorption correction was then applied using the XEMP program[27] before hydrogen atoms were introduced in calculated positions riding on the carbon atoms, and all non-hydrogen atoms allowed to refine anisotropically. The three highest peaks in the difference map were modelled as a molecule of ethanol in the final refinement and immediately assigned anisotropic thermal parameters. The hydroxy hydrogen atom was placed in a calculated position and a peak at ≈ 1 Å from the ethanol oxygen was discounted because of poor geometry. The final refinement converged at $R1 = 0.0413$ [$wR2 = 0.0810$ for 6089 data with $I > 2\sigma(I)$, and $R1 = 0.0658$ ($wR2 = 0.0925$) for all 7958 data]. The maximum residual density was 1.18 e $Å^{-3}$.

$[Cu_2L^1][O_3SCF_3]_2$ 3. *Crystal data.* $C_{32}H_{36}Cu_2F_6N_8O_6S_5$, $M = 1030.07$, orange plate, crystal dimensions 0.90 × 0.42 × 0.12 mm, orthorhombic, space group *Pcca*, $a = 28.464(5)$, $b = 15.616(4)$, $c = 18.459(2)$ Å, $U = 8205(3)$ $Å^3$, $\mu = 1.372$ mm^{-1}, $D_c = 1.67$ g cm^{-3}, $Z = 8$, $F(000) = 4192$.

Unit-cell parameters were determined by non-linear least-squares refinement of 40 accurately centred reflections ($10 < 2\theta < 25°$). Data were collected at 133 K on a Siemens P4 four-circle diffractometer using graphite-monochromated Mo-Kα radiation (λ = 0.710 73 Å). Using 1.4° ω scans at 7° min^{-1}, 4593 unique reflections were collected in the range $4 < 2\theta < 45°$. Crystal stability was monitored by recording three check reflections every 97 and no significant variation was observed. The data were corrected for Lorentz-polarisation effects and an empirical absorption correction was applied based on ψ-scan data ($T_{max} = 1.00$, $T_{min} = 0.821$).

The structure was solved by direct methods[25] which revealed most of the non-hydrogen atoms and the remaining atoms were located from Fourier-difference maps. All non-hydrogen atoms were refined with anisotropic atomic displacement parameters. Hydrogen atoms were inserted at calculated positions with isotropic thermal parameters riding on the equivalent isotropic displacement parameters of their carrier atoms. All the data were used for refinement of 533 parameters on F^2 which converged with $wR2 = 0.2078$, goodness of fit = 0.970 (all data) and conventional $R1 = 0.0726$ [for $I > 2\sigma(I)$]. The final difference map showed no significant residual electron density except for two peaks of *ca.* 1.8 e $Å^{-3}$ close to Cu(1) which are dependent on the parameters used for the (thin plate) absorption correction.[27] All programs used on the structure refinement are contained in the SHELXL 93[26] package.

Table 7 Magnetic parameters

Complex	μ/μ_B 80	μ/μ_B 298 K	$-2J/cm^{-1}$	g	R
5	1.35	1.68	72	2.00	7.3×10^{-4}
7	2.03	2.04	−5	2.31	1.4×10^{-3}
6	1.17	1.72	112	2.15	2.1×10^{-3}
5′ (aged)	1.52	1.69	44	1.96	2.4×10^{-3}

Atomic coordinates, thermal parameters, and bond lengths and angles have been deposited at the Cambridge Crystallographic Data Centre (CCDC). See Instructions for Authors, *J. Chem. Soc., Dalton Trans.*, 1996, Issue 1. Any request to the CCDC for this material should quote the full literature citation and the reference number 186/87.

INEPT spectra

These were obtained at 18.62 MHz and at 294 and 228 K. The dephasing delay was 0.294 s in a standard experiment, typically requiring 2000–20 000 transients.

Magnetic susceptibility measurements

Magnetic susceptibility measurements were made in the temperature range 80–300 K using an Oxford Instruments Faraday balance with a field of 0.8 T. Mercury tetrakis(thiocyanato)cobaltate(II) was used to calibrate the balance, and all molar susceptibilities were corrected for diamagnetic contribution using Pascal's constants. The data (See SUP 57144) were fitted by the Bleaney–Bowers equation (1), which expresses the

$$\chi_m = (Ng^2\beta^2/3kT)[1 + \tfrac{1}{3}\exp(-2J/kT)]^{-1} + N_\alpha \quad (1)$$

variation of the molar susceptibility with temperature for the spin Hamiltonian $H = -2J(S_1 \cdot S_2)$. The value of the temperature-independent paramagnetism, N_α, was set at 60×10^{-6} cm^3 mol^{-1} per copper ion. The values of J and g were (Table 7) determined by least-squares fitting with an agreement factor $R = \Sigma_i[\chi_m(\text{exptl.})(i) - \chi_m(\text{calc.})(i)]^2/[\chi_m(\text{exptl.})(i)]^2$.

Acknowledgements

We thank the Open University Research Committee and the SERC for support (to D. J. M., G. G. M. and Q. L.) and also the SERC for access to services (High-field NMR at Warwick and FAB mass spectrometry at Swansea).

References

1 E. T. Adman, *Adv. Protein Chem.*, 1991, **42**, 145.
2 G. W. Canters and G. Gilardi, *FEBS Lett.*, 1993, **325**, 39.
3 E. Danielsen, R. Bauer, L. Henningsen, M.-L. Andersen, M. J. Bjerrum, T. Butz, W. Troger, G. W. Canters, C. W. G. Hoitink, G. Karlsson, O. Hansson and A. Messerschmidt, *J. Biol. Chem.*, 1995, **270**, 573.

4 M. G. B. Drew, J. Hunter, D. J. Marrs, C. J. Harding and J. Nelson, *J. Chem. Soc., Dalton Trans.*, 1992, 3235.
5 D. J. Marrs, V. McKee, J. Nelson, Q. Lu and C. J. Harding, *Inorg. Chim. Acta*, 1993, **211**, 195.
6 Q. Lu, J.-M. Latour, C. J. Harding, N. Martin, D. J. Marrs, V. McKee and J. Nelson, *J. Chem. Soc., Dalton Trans.*, 1994, 1471; C. Harding, Q. Lu, V. McKee and J. Nelson, *J. Chem. Soc., Chem. Commun.*, 1993, 1768.
7 Q. Lu, D. J. Marrs, J. F. Malone, V. McKee, C. J. Harding and J. Nelson, *J. Chem. Soc., Dalton Trans.*, 1995, 1739.
8 C. J. Harding, V. McKee and J. Nelson, *J. Am. Chem. Soc.*, 1991, **113**, 9684.
9 Q. Lu, V. McKee and J. Nelson, *J. Chem. Soc., Chem. Commun.*, 1994, 649.
10 M. McCann, J. Nelson and Q. Lu, *J. Inorg. Biochem.*, 1993, **51**, 633.
11 R. Louis, Y. Agnus and R. Weiss, *J. Am. Chem. Soc.*, 1977, **99**, 8502.
12 A. J. Blake, D. Collison, R. O. Gould, G. Reid and M. Schroder, *J. Chem. Soc., Dalton Trans.*, 1993, 521; A. J. Blake, R. O. Gould, C. Rodek, A. Taylor and M. Schroder, *Chemistry of Copper and Zinc Triads*, Special Publ. 131, Royal Society of Chemistry, Cambridge, 1993 and refs. therein; M. G. B. Drew, C. Cairns, A. Lavery and S. M. Nelson, *J. Chem. Soc., Chem. Commun.*, 1980, 1122.
13 P. C. Yates, M. G. B. Drew, J.-T. Grimshaw, K. P. McKillop, S. M. Nelson, P. T. Ndifon, C. A. McAuliffe and J. Nelson, *J. Chem. Soc., Dalton Trans.*, 1991, 1973; M. G. B. Drew, P. C. Yates, J.-T. Grimshaw, A. Lavery, K. P. McKillop, S. M. Nelson and J. Nelson, *J. Chem. Soc., Dalton Trans.*, 1988, 347; N. A. Bailey, M. M. Eddy, D. E. Fenton, S. Moss, A. Mukhopadhyay and G. Jones, *J. Chem. Soc., Dalton Trans.*, 1984, 2281.
14 B. Dietrich, J.-M. Lehn and J.-P. Sauvage, *Chem. Commun.*, 1970, 1055; L. R. Gahan, G. A. Lawrance and A. M. Sargeson, *Inorg. Chem.*, 1982, **21**, 2699; P. Bernhard, D. A. Bull, W. T. Robinson and A. M. Sargeson, *Aust. J. Chem.*, 1992, **45**, 1241 and refs. therein.
15 V. McKee, W. T. Robinson, D. McDowell and J. Nelson, *Tetrahedron Lett.*, 1989, 7543.
16 M. G. B. Drew, J. Hunter, D. J. Marrs and J. Nelson, *J. Chem. Soc., Dalton Trans.*, 1992, 11; M. G. B. Drew, D. McDowell and J. Nelson, *Polyhedron*, 1988, 2229.
17 R. Abidi, F. Arnaud-Neu, M. G. B. Drew, D. J. Marrs, J. Nelson and M.-J. Schwing-Weil, *J. Chem. Soc., Perkin Trans. 2*, in the press.
18 G. C. van Stein, G. van Koten, K. Vrieze, A. L. Spek, E. A. Klop and C. Brevard, *Inorg. Chem.*, 1985, **24**, 1367 and refs. therein.
19 C. J. Harding, F. E. Mabbs, V. McKee and J. Nelson, *J. Chem. Soc., Dalton Trans.*, in the press.
20 G. M. Sheldrick, SHELX 76, University of Cambridge, 1976.
21 J. M. Griffing and L. F. Salisburg, *J. Am. Chem. Soc.*, 1948, **70**, 3416.
22 T. Stone, *Bull Chem. Soc. Jpn.*, 1964, **37**, 1197.
23 J. Chin, M. Banaszczyk, V. Jubian and X. Zou, *J. Am. Chem. Soc.*, 1989, **111**, 186.
24 J. L. Van Winkle, J. D. McClure and P. H. Williams, *J. Org. Chem.*, 1966, **31**, 3300.
25 G. M. Sheldrick, SHELXS 86, *Acta Crystallogr., Sect. A*, 1990, **46**, 467.
26 G. M. Sheldrick, SHELXL 93, University of Göttingen, 1993.
27 G. M. Sheldrick, *SHELXTL PC Users Manual*, Siemens Analytical X-Ray Instruments, Madison, WI, 1990.

Received 7*th December* 1995; *Paper* 5/07997G